European Journal of Immunology

Supporting Information

for

DOI 10.1002/eji.201646297

Jakob Zimmermann, Thomas Hübschmann, Florian Schattenberg, Joachim Schumann, Pawel Durek, René Riedel, Marie Friedrich, Rainer Glauben, Britta Siegmund, Andreas Radbruch, Susann Müller and Hyun-Dong Chang

High-resolution microbiota flow cytometry reveals dynamic colitis-associated changes in fecal bacterial composition

© 2016 The Authors. *European Journal of Immunology* published by WILEY-VCH Verlag GmbH & Co. KGaA, Weinheim.

European Journal of Immunology

Supporting Information

for

DOI 10.1002/eji.201646297

Jakob Zimmermann, Thomas Hübschmann, Florian Schattenberg, Joachim Schumann, Pawel Durek, René Riedel, Marie Friedrich, Rainer Glauben, Britta Siegmund, Andreas Radbruch, Susann Müller and Hyun-Dong Chang

High-resolution microbiota flow cytometry reveals dynamic colitis-associated changes in fecal bacterial composition

© 2016 The Authors. *European Journal of Immunology* published by WILEY-VCH Verlag GmbH & Co. KGaA, Weinheim.

European Journal of Immunology

Supporting Information

for

DOI 10.1002/eji.201646297

Jakob Zimmermann, Thomas Hübschmann, Florian Schattenberg, Joachim Schumann, Pawel Durek, René Riedel, Marie Friedrich, Rainer Glauben, Britta Siegmund, Andreas Radbruch, Susann Müller and Hyun-Dong Chang

High-resolution microbiota flow cytometry reveals dynamic colitis-associated changes in fecal bacterial composition

© 2016 The Authors. *European Journal of Immunology* published by WILEY-VCH Verlag GmbH & Co. KGaA, Weinheim.

European Journal of Immunology

Supporting Information

for

DOI 10.1002/eji.201646297

Jakob Zimmermann, Thomas Hübschmann, Florian Schattenberg, Joachim Schumann, Pawel Durek, René Riedel, Marie Friedrich, Rainer Glauben, Britta Siegmund, Andreas Radbruch, Susann Müller and Hyun-Dong Chang

High-resolution microbiota flow cytometry reveals dynamic colitis-associated changes in fecal bacterial composition

© 2016 The Authors. *European Journal of Immunology* published by WILEY-VCH Verlag GmbH & Co. KGaA, Weinheim.

Supporting Information

High-resolution flow cytometry to determine dynamic colitis-associated changes in the fecal microbiota

Jakob Zimmermann[1*], Thomas Hübschmann[2*], Florian Schattenberg[2], Joachim Schumann[2], Pawel Durek[1], Marie Friedrich[3], Rainer Glauben[3], Britta Siegmund[3], Andreas Radbruch[1], Susann Müller[2**] & Hyun-Dong Chang[1**]

1) German Rheumatism Research Center Berlin (DRFZ), an institute of the Leibniz Association, Berlin, Germany
2) Helmholtz Center for Environmental Research (UFZ), Department for Environmental Microbiology, Leipzig, Germany
3) Charité - Universitätsmedizin Berlin, Medical Department (Gastroenterology, Infectious Diseases, Rheumatology), Campus Benjamin Franklin, Berlin

*) These authors contributed equally to this work.

**) These authors contributed equally to this work as senior co-authors.

Corresponding author: Dr. rer. nat. Hyun-Dong Chang, chang@drfz.de

This Supporting Information contains seven figures, the captions for the two supplementary tables and detailed methodology.

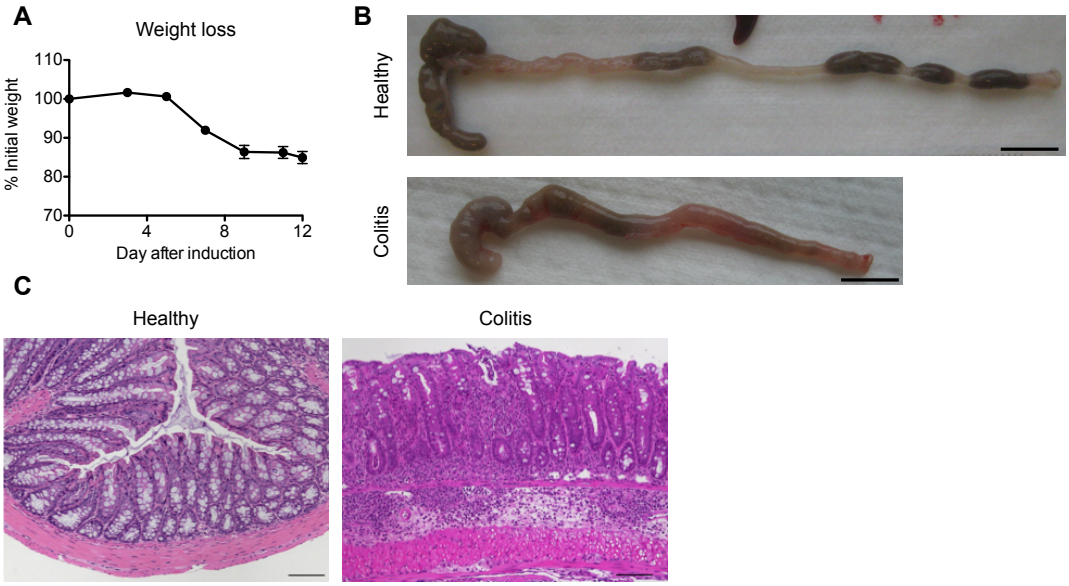

Supporting Information Figure 1. T cell transfer colitis results in weight loss, diarrhea and histological signs of colitis. Colitis was induced by i.v. transfer of $4x10^5$ CD4+CD45RB^{hi} T cells into *Rag1*$^{-/-}$ recipients. (A) Weight loss relative to starting weight for n = 4 mice from one representative experiment. (B) Macroscopic picture of healthy colon and after induction of T cell transfer colitis (day 12-15, bars are 1 cm). (C) Hematoxylin and eosin-stained colon section from a healthy mouse and one with T cell transfer colitis (day 12-15, bars are 100 µm).

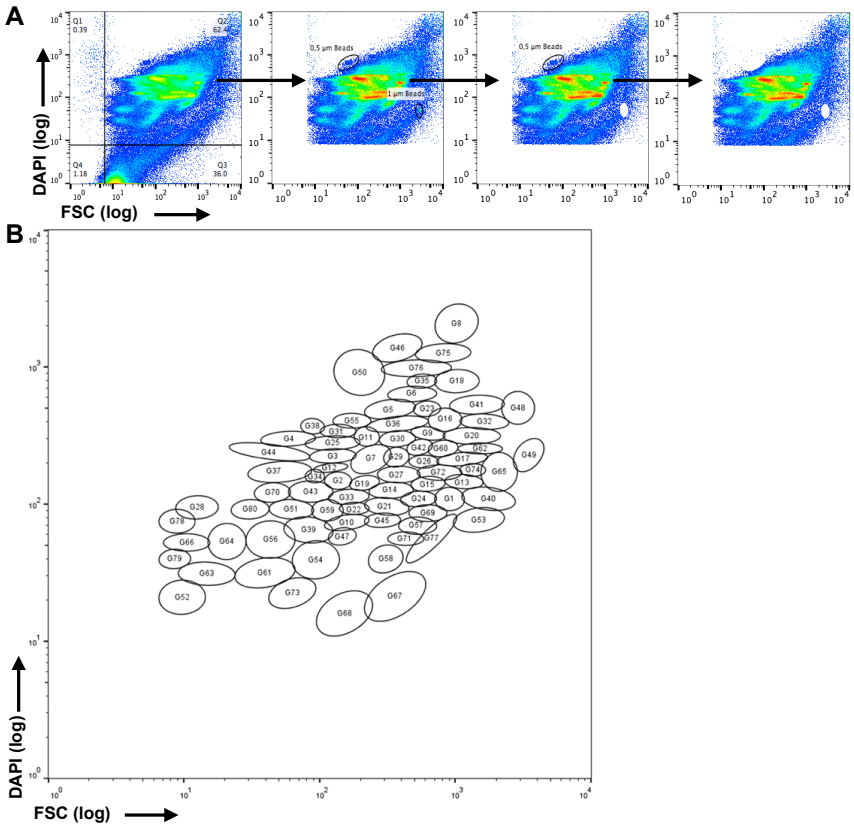

Supporting Information Figure 2. Gating strategy and electronic gates used for the quantification of populations of the fecal microbiota. (A) Representative illustration of the gating strategy for the flow cytometric analysis of fecal bacteria. After exclusion of electronic noise (Q1, Q4) and DAPI negative events (Q3), spiked in 0.5 µm and 1 µm control beads were consecutively excluded from the analysis. (B) For cytometric barcoding (CyBar) analysis, electronic gates were set for all individual samples by an operator. Individual gates were consolidated into one single gate template for all analyses in this study. Relative frequencies of events within the gates were used for further analysis.

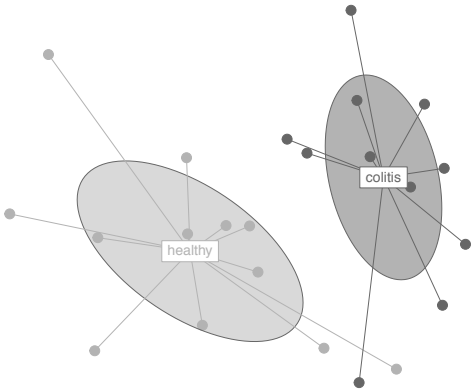

Supporting Information Figure 3. CHIC analysis of the microbiota from colitic and healthy mice. Non-metric, multidimensional scaling (NMDS) plot of fecal samples of 12 healthy and 11 colitic mice (same as for Fig. 1) analyzed by cytometric histogram image comparison (CHIC) [1].

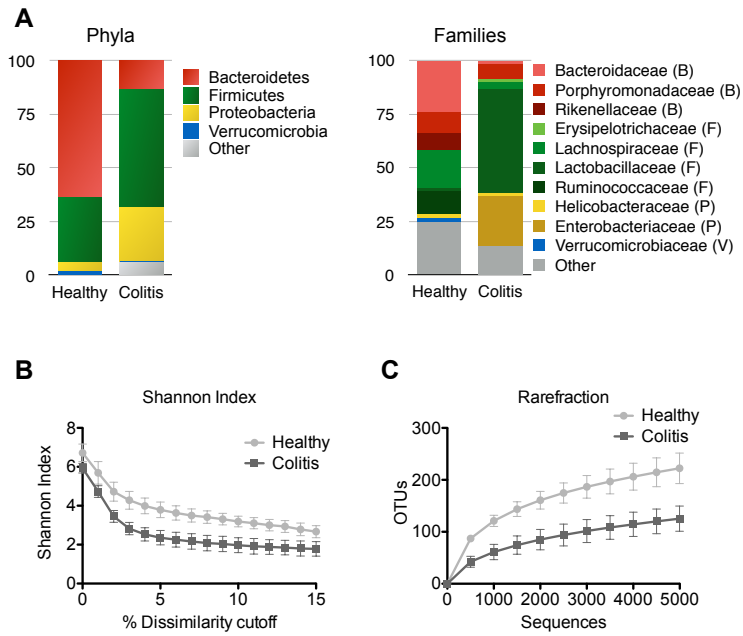

Supporting Information Figure 4. T cell transfer colitis results in severe dysbiosis. Colitis was induced by i.v. transfer of $4x10^5$ CD4+ $CD45RB^{hi}$ T cells into *Rag1*$^{-/-}$ recipients. The fecal microbiota was analyzed before and during established colitis (days 12–15). 16s rDNA from unsorted fecal bacteria of n=3 individual mice before and after the onset of colitis was analyzed by next generation sequencing and with the ribosomal database project (RDP) as outlined in materials and methods. (A) Median frequencies on the phylum and family level with characters in parenthesis specifying the phylum of each family (B = *Bacteroidetes*, F = *Firmicutes*, P = *Proteobacteria*, V = *Verrucomicrobiae*). Taxa below 1% were summarized as "other". (B) Shannon index as a function of the dissimilarity cutoff used for clustering calculated with RDP. Mean ± SEM for n = 3 mice. (C) Rarefraction analysis showing the number of different operational taxonomic units (OTUs) as a function of the number of sequences analyzed calculated with RDP. Mean ± SEM for n = 3 mice. Experiment was performed once.

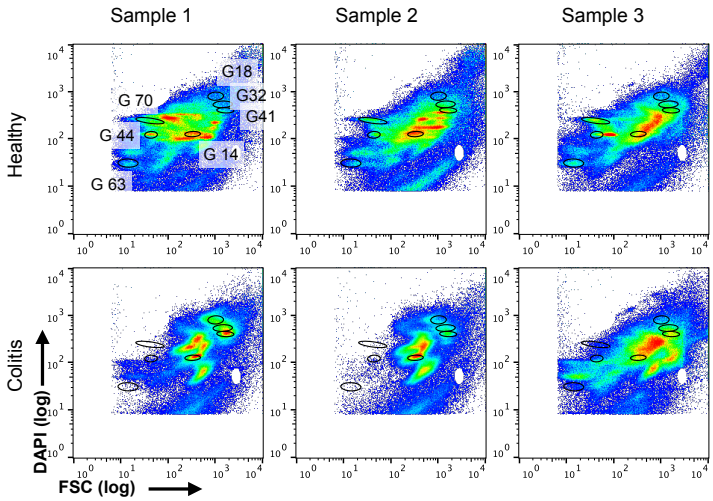

Supporting Information Figure 5. Overview of sorted populations from healthy and colitic mice. Exemplary populations were sorted by FACS from n=3 individual mice before and/or after the onset of T cell transfer colitis.

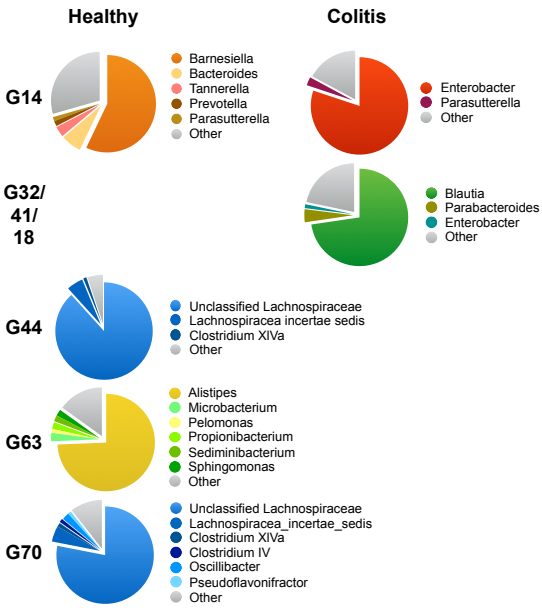

Supporting Information Figure 6. Detailed phylogenetic composition of sorted populations. The 16s rDNA sequences of sorted bacterial populations were analyzed before and/or after the onset of T cell transfer colitis for n=3 individual mice (same individuals as in Fig. 2). Median composition of gates 14, 32/41/18, 44, 63, and 70 on the genus level. Unclassified or low abundance genera (<1%) were referred to as “Other”. Experiment was performed once.

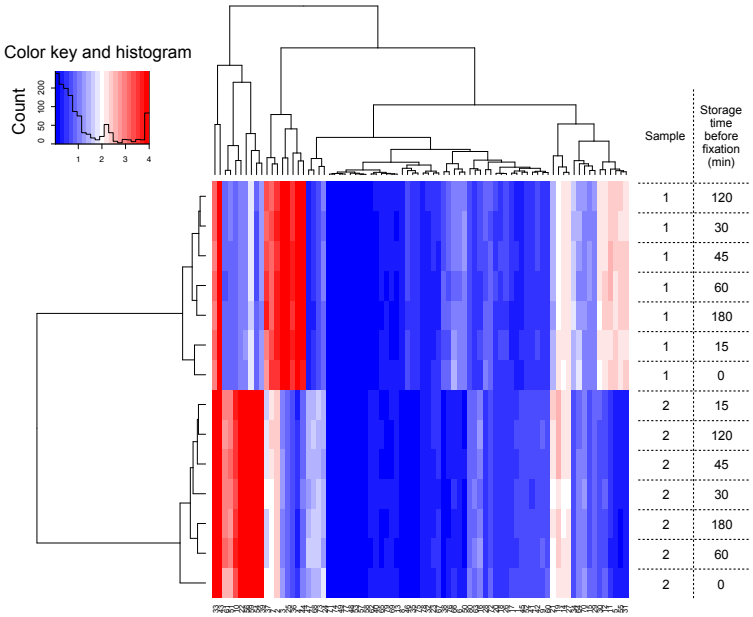

Supporting Information Figure 7. Minimal impact of storage duration on the FSC/DAPI pattern of the fecal microbiota. For n=2 individual mice, one fecal pellet was collected, minced, filtered and the suspension was kept on ice in PBS for the indicated amount of time before fixation with 2% formaldehyde. Frequencies of bacteria in cytometric gates were analyzed by flowCyBar as outlined in materials and methods. Frequencies of bacteria are indicated by color: blue (0-2%), white (2%), and red (more than 2%). Similar samples are connected by hierarchical clustering. Experiment was performed once.

Supporting Information File 2. Frequencies of bacteria in cytometric gates. Depicted are frequencies of bacteria in the electronic gates of the gating template (Supporting Information Fig. 2B) for all analyzed experiments and samples.

Supporting Information File 3. 16s rDNA sequencing: copy number-adjusted read counts. Sequencing results were analyzed with the Ribosomal Database Project (RDP) “Classifier” tool at a confidence threshold of 50. Given are copy number-adjusted read counts.

Materials and Methods

Mice

C57BL/6J & *Rag1*$^{-/-}$ mice were purchased from the Charles River laboratories and housed in individually ventilated cages under specific pathogen-free conditions according to FELASA standards. Specifically, mice from this facility have been tested positive for *Helicobacter bilis* (*H. bilis*), *H. hepaticus*, and *H. typhlonicus*, as well as murine norovirus and *Pneumocystis murina* but are free of any obligate mouse pathogens. Before T cell transfer, *Rag1*$^{-/-}$ were colonized by oral gavage with a complex bacterial suspension from donor feces tested positive for segmented filamentous bacteria (SFB) and *Helicobacter spp*. (*H. spp*). Successful colonization was confirmed by PCR from fecal DNA with the following primer pairs: H. spp [2]: forward: 5'-ctatgacgggtatccggc-3', reverse: 5'-attccacctacctctccca-3'. SFB [3]: forward: 5'-gacgctgaggcatgagagcat-3', reverse: 5'-gacggcacggattgttattca-3'. Mice were handled in accordance with good animal practice as defined by the German animal welfare bodies. All experiments were approved by the regulatory office „Landesamt für Gesundheit und Soziales" in Berlin, Germany (permit number G0300/11).

Colitis induction

Colitis was induced as published before [4]. Briefly, CD4+ T cells from spleen and pLN of C57BL/6J donors were purified by high-gradient magnetic cell sorting (MACS) using mouse CD4 direct beads (L3T4, Miltenyi Biotec, Bergisch Gladbach, Germany). Viable $CD4^{+}CD45RB^{hi}$ cells were isolated by fluorescence-activated cell sorting (FACS) with a FACSAria I (BD Biosciences, Heidelberg, Germany). $4x10^{5}$ cells were injected i.v. into each *Rag1*$^{-/-}$ recipient. Mice were sacrificed 2-3 weeks after transfer, when signs of diarrhea and weight loss became apparent. Diarrhea was scored in a blinded fashion with 1 = solid, dark; 2 = soft, dark; 3 = mushy, light; 4 = liquid.

Isolation of fecal bacteria

Fecal pellets were freshly harvested and immediately stored in ice-cold PBS. FSC/DAPI profiles remained stable for at least 3 h before fixation (Supporting Information Fig. 7). Following mincing with a razor blade, the bacterial

suspension was separated from large particles by filtering through a 70 µm mesh. After centrifugation for 5 min at 3000 g at 4 °C, fecal bacteria were fixed with 2% formaldehyde for 30 min at room temperature. Following washing with PBS, fecal bacteria were resuspended in 70% ethanol and stored at -20°C until further analysis.

Staining of bacteria

Bacteria were stained as described before [5]. Briefly, samples were vortexed vigorously for 10 s and adjusted to an optical density of 0.035 (dλ700nm = 0.5 cm) with PBS. One mL of the adjusted solution was centrifuged (3200 g, 10 min, 4 °C). The pellet was resuspended in 0.5 mL of solution A (0.11 M citric acid, 4.1 mM Tween 20 in bidistilled water) and incubated for 20 min. After another centrifugation step the pellet was resuspended in solution B (0.5 µM 4′,6-diamidino-2′-phenylindole (DAPI, SIGMA), 400 mM Na_2HPO_4 /NaH_2PO_4, pH 7.0) and incubated in the dark for 3 h. All samples were filtered through 50 µm CellTrics® (Partec, Münster, Germany) prior to cytometric measurement. Fluorescence beads Fluoresbrite BB Carboxylate microspheres 0.5 µm (360/407, Lot-Nr. 552744, Polyscience, USA) and XPR 1528-Polymer Microspheres 1 µm (350/530, Lot-Nr. 5866, ThermoScientific, USA) were added to each sample as internal benchmark for standardized FSC and fluorescence amplification (Supporting Information Fig 2A). For all measurements 250.000 stained cells were recorded.

Flow cytometry and cell sorting

Samples were measured as described before[5]. Briefly, cytometric measurements were performed with a MoFlo cell sorter (DakoCytomation, USA) equipped with a 488 nm argon laser (400 mW) and a ML-UV laser (333-365 nm, 100 mW). Very similar distributions were obtained, but are not shown in this study, with an Influx cell sorter (BD) and a CyFlow analyser (Sysmex-Partec) without a sort option. We recommend a UV laser as excitation source with a power output of at least 50 mW and an alignment of the used cytometer in such a way that an exclusive scatter pattern of bacteria (FCS/SSC) apart from instrumental noise can be obtained. In this study excitation at 488 nm was used to analyze forward scatter (FSC, 488/10) and side scatter (SSC,

trigger signal, 488/10), and the ML-UV (450/65) to measure DAPI-DNA fluorescence. Photomultiplier tubes were obtained from Hamamatsu Photonics (models R928 and R3896; 211 Hamamatsu City, Japan). Fluorescent beads FluoSpheres 2 µm (505/515, Lot-Nr. 24498W, Molecular Probes Eugene, Oregon, USA), FluoSpheres 1 µm (350/440, Lot-Nr. 69A1-1, Molecular Probes Eugene, Oregon, USA), and Fluoresbrite BB Carboxylate microspheres 0.5 µm (360/407, Lot-Nr. 552744, Polyscience, USA) were used to align the instrumental settings. Cytometric data acquisition was performed with Summit (version 4.3, DakoCytomation, USA) and FlowJo (version 10, FlowJo LLC, Oregon, USA). A bead template was created to align cytometric data over long time periods (Supporting Information Fig. 2B). The flow cytometric data files are deposited in the FlowRepository database (www.flowrepository.org) with the repository IDs FR-FCM-ZZP6 (colitis) and FR-FCM-ZZP8 (PBS storage stability).

Cell sorting was performed using the most accurate sort mode (single and one drop mode: highest purity 99%, 8000 cells per second) using either a two-way- or a four-way-sort option at high speed (12 m s^{-1}). Per sample and gate, 500.000 cells were collected for 16s rDNA sequencing.

DNA isolation and sequencing of 16s rDNA

DNA from sorted bacteria was isolated as published before [6]**.** Briefly, pellets of bacterial cells were resuspended in 10% Chelex, vortexed briefly and incubated at 95 °C for 45 min. After centrifugation at 7000 g and 4 °C for 5 min, the supernatant containing genomic DNA was frozen at -20 °C until further analysis. Sequencing of the 16s rDNA was performed by LGC Genomics, Berlin, Germany.

16s rDNA templates were amplified by PCR using the total DNA of $2.5x10^5$ bacterial cells. The PCR included 15 pmol of each forward primer 341F 5'-NNNNNNNNNNTCCTACGGGNGGCWGCAG and reverse primer 785R 5'-NNNNNNNNNNTGACTACHVGGGTATCTAAKCC in 20 µL volume of MyTaq buffer containing 1.5 units MyTaq DNA polymerase (Bioline) and 2 µl of BioStabII PCR Enhancer (Sigma). For each sample, the forward and reverse primers had the same 10-nt barcode sequence. PCRs were carried out for 30 cycles using the following parameters: 2 min 96 °C pre-denaturation; 96 °C for

15 s, 50 °C for 30 s, 70 °C for 90 s. DNA concentration of amplicons of interest was determined by gel electrophoresis. Twenty ng amplicon DNA of each sample were pooled for up to 48 samples carrying different barcodes. If needed, PCRs showing low yields were further amplified for 5 cycles. The amplicon pools were purified with one volume AMPure XP beads (Agencourt) to remove primer dimers and other small mispriming products, followed by an additional purification on MinElute columns (Qiagen). About 100 ng of each purified amplicon pool DNA was used to construct Illumina libraries using the Ovation Rapid DR Multiplex System 1-96 (NuGEN). Illumina libraries were pooled and size selected by preparative gel electrophoresis. Sequencing was done on an Illumina MiSeq using V3 Chemistry (Illumina). For the analysis, reads were de-multiplexed using Illumina's CASAVA data analysis software and the barcode sequence was clipped after sorting. Reads with missing barcodes, one-sided barcodes or conflicting barcode pairs were discarded. Illumina TruSeqTM adapters were clipped in all reads. Reads with final length < 100 bases were discarded. Primers were detected and clipped with 3 mismatches being allowed per primer. Forward and reverse reads were combined using BBMerge 34.48 (http://bbmap.sourceforge.net/). Raw sequence data were deposited at the NCBI Sequence Read Archive (SRA) under the accession number SRP069847.

Combined reads were classified using the ribosomal database project “Classifier” tool with a confidence cutoff of 50% [7]. Charts were generated using the copy number-adjusted numbers of reads as a frequency of the overall number of reads mapped to the kingdom Bacteria.

For the calculation of the Shannon index and the rare fraction analysis, the RDP pipeline was used including the tools “Alignment”, “Complete Linkage Clustering”, “Shannon & Chao1 index”, and “Rarefraction” using 5000 reads per sample [8].

Statistical analysis

Flow cytometry data were analysed using Cytometric Barcoding, as described by Koch et al. [5, 9] with the R package flowCyBar [10]. Briefly, electronic gates were set in all individual samples of the whole study to accommodate all occurring populations. Gates were consolidated into one general gating

template that was used for all the samples of this study (Supporting Information Fig. 2B). Charts were created with the frequencies of bacteria in these gates. Differences in frequencies were tested for statistical significance the student's t test for independent samples followed by Benjamini-Hochberg adjustment of the false discovery rate (Fig. 1B). The abundance variations of the relative cell numbers per gate are shown as a vertical boxplot (Fig. 1B). Barcodes display the frequencies for each gate at the indicated color code (Supporting Information Fig. 7). The plots were generated with the R-script "cybar_plot" of the R-package flowCyBar. Both gates and samples were ordered and clustered by hierarchical clustering using the Euclidean distance. The distance of the edges connecting 2 nodes in the dendrograms represents the dissimilarity between 2 clusters. We used the method "nmds" of the R-package flowCyBar (Fig. 1C) for calculating the pairwise distances between all samples with Bray-Curtis dissimilarity as distance measure and for creating non-metric multidimensional scaling (NMDS) plots based on the relative frequencies of bacteria in each gate. CHIC was performed as described previously [1].

Supporting Information References

1. **Koch, C. et al.,** *Cytometry*. 2013; **83A**:561–567.DOI: 10.1002/cyto.a.22286.

2. **Riley, LK. et al.,** *Journal of Clinical Microbiology*. 1996; **34**:942–946.

3. **Barman, M. et al.,** *Infection and Immunity*. 2008; **76**:907–915.DOI: 10.1128/IAI.01432-07.

4. **Powrie, F. et al.,** *Int Immunol*. 1993; **5**:1461–1471.

5. **Koch, C. et al.,** *Environ. Sci. Technol.* 2013:130108105239000.DOI: 10.1021/es3041048.

6. **Koch, C. et al.,** *Nature Protocols*. 2013; **8**:190–202.DOI: 10.1038/nprot.2012.149.

7. **Wang, Q. et al.,** *Applied and Environmental Microbiology*. 2007; **73**:5261–5267.DOI: 10.1128/AEM.00062-07.

8. **Cole, JR. et al.,** *Nucleic Acids Research*. 2014; **42**:D633–D642.DOI: 10.1093/nar/gkt1244.

9. **Koch, C. et al.,** *Front Microbiol*. 2014; **5**:273.DOI: 10.3389/fmicb.2014.00273.

10. **Schumann, J. et al.,** flowCyBar-Analyze flow cytometric data using gate information. 2014.